

## Nonclassical Carbocations as C–H Hydrogen Bond Donors

Mihaela D. Bojin and Dean J. Tantillo\*

Department of Chemistry, University of California, Davis, One Shields Avenue, Davis, California 95616

Received: November 30, 2005; In Final Form: February 18, 2006

Computed [B3LYP/6-31+G(d,p) and MP2/6-31+G(d,p)] structures and binding energies for complexes of nonclassical cations (carbonium ions) with ammonia, in the gas phase and several solvents, are described. Overall, nonclassical cations are found to be competent C–H hydrogen bond donors. The potential relevance of the C–H $\cdots$ N interactions holding the carbocation $\cdot$ amine complexes together for enzyme-catalyzed terpenoid synthesis is discussed.

### Introduction

Can nonclassical carbocations (i.e., carbonium ions)<sup>1</sup> exist in enzyme active sites? The answer to this question is of fundamental importance to the field of natural product biosynthesis due to the prevalence of carbocations in the putative mechanisms for terpenoid biosynthesis via terpenoid synthases.<sup>2</sup> This is an extremely complicated question, however, whose answer depends on many different factors. Two of these factors are addressed herein using computational quantum chemistry. First, we address the question of whether basic/nucleophilic molecules such as ammonia (a simple model of enzyme active site residues such as lysine and histidine) will perturb the structures of nonclassical ions through C–H $\cdots$ X interactions (X = heteroatom with lone pair);<sup>3–5</sup> that is, will such interactions change a preference for a nonclassical structure into a preference for a classical structure? Second, we compare the strengths of C–H $\cdots$ X interactions (here, X = N) for which the C–H units are part of carbocations to other C–H $\cdots$ X interactions.

### Methods

All calculations were performed with GAUSSIAN03.<sup>6</sup> Geometries were optimized without symmetry constraints using the hybrid Hartree–Fock/density functional theory (HF/DFT) B3LYP/6-31+G(d,p) method<sup>7</sup> as well as the MP2/6-31+G(d,p) method.<sup>8</sup> Recent reports have compared the performance of the B3LYP and MP2 methods in computing geometries and relative energies of delocalized carbocations.<sup>9</sup> In general, discrepancies between the two methods tend to occur when the potential energy surface in the vicinity of a given structure is flat. Such discrepancies can be viewed as problems, but they also serve as markers for cases where intervention by noncovalent interactions or dynamic effects may control the structures formed in a given reaction. In addition, while density functional methods such as B3LYP are often suitable for describing hydrogen bonds (since these are largely electrostatic in nature),<sup>10</sup> MP2 is generally more appropriate than DFT for describing noncovalent interactions that are more dependent on dispersion interactions (for example,  $\pi$ – $\pi$  stacking).<sup>11</sup> The use of diffuse functions with density functional calculations was also recently discussed.<sup>12</sup>

All stationary points were characterized by frequency calculations, and reported energies include zero-point energy correc-

tions (unscaled). In some cases, the synchronous transit-guided quasi-Newton (STQN) method, which searches for a transition state structure between specified reactant and product structures (QST2),<sup>13</sup> was used to help locate transition structures. For several transition structures, intrinsic reaction coordinate calculations<sup>14</sup> were also used to verify their nature.

Interaction energies for various structures were computed as the difference in zero-point-corrected energies for complexes and the sum of the energies for the separate components (entropies are not included). Corrections to these complexation energies for basis set superposition error were computed for all complexes and are included in all reported interaction energies.<sup>15</sup> These corrections are typically  $\leq 1.9$  kcal/mol for our B3LYP/6-31+G(d,p) calculations and  $\leq 2.2$  kcal/mol for our MP2/6-31+G(d,p) calculations. Herein, negative interaction energies indicate exothermic complex formation.

Structures were also reoptimized at the B3LYP/6-31+G(d,p) level using the CPCM solvation model with UAKS radii.<sup>16,17</sup> Continuum dielectric environments corresponding to three different solvents were used as follows: benzene ( $\epsilon = 2.247$ ), a typical nonpolar solvent and mimic of the hydrophobic cavities often found in terpenoid synthase active sites;<sup>18</sup> nitromethane ( $\epsilon = 38.2$ ), a moderately polar solvent; and water ( $\epsilon = 78.39$ ), a very polar solvent and a very simplified model of aqueous solution (the setting for most “background” reactions in biology). Structural drawings were produced using Ball & Stick.<sup>19</sup>

### Results and Discussion

As part of a research program on the mechanisms of enzyme-catalyzed carbocation rearrangements,<sup>9c</sup> we are examining complexes of nonclassical species with small models of protein residues.<sup>20</sup> While various types of enzyme–nonclassical carbocation interactions that take advantage of the charge distribution in these cations are possible (Figure 1),<sup>21</sup> we focus herein on complexes with ammonia, a simple model of potentially basic/nucleophilic residues such as histidine and lysine.<sup>22–26</sup>

**Small Representative Systems in the Gas Phase.** Various C<sub>2</sub>H<sub>5</sub><sup>+</sup>, C<sub>3</sub>H<sub>7</sub><sup>+</sup>, and C<sub>4</sub>H<sub>9</sub><sup>+</sup> isomers were characterized in both the presence and the absence of NH<sub>3</sub>. Structures were located using both the B3LYP/6-31+G(d,p) and the MP2/6-31+G(d,p) methods.<sup>7,8</sup> Nonclassical minima (bridged cations with hypercoordinate carbons or hydrogens)<sup>1</sup> for the C<sub>2</sub>H<sub>5</sub><sup>+</sup>, C<sub>3</sub>H<sub>7</sub><sup>+</sup>, and C<sub>4</sub>H<sub>9</sub><sup>+</sup> series are shown in Figure 2. These uncomplexed cations have been studied previously at various levels of theory,<sup>27</sup> so only a few comments on their structures are included here.

\* To whom correspondence should be addressed. E-mail: tantillo@chem.ucdavis.edu.

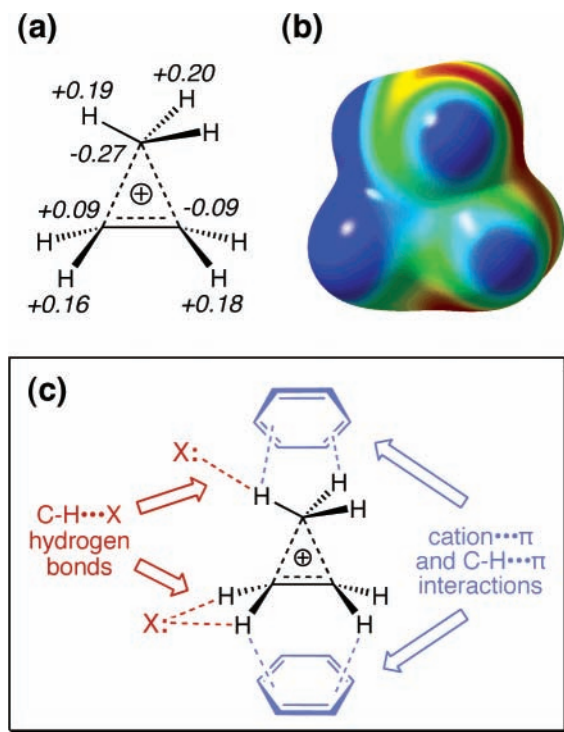


**Figure 1.** (a) Computed (B3LYP/6-31+G(d,p), CHelpG<sup>21</sup>) charges for the bridged isomer of  $C_3H_7^+$ , a representative nonclassical cation. (b) Electrostatic potential surface (red is least positive, and blue is most positive; the range is +0.20 to +0.27 au). (c) Potential interactions between nonclassical carbocations and active site residues.

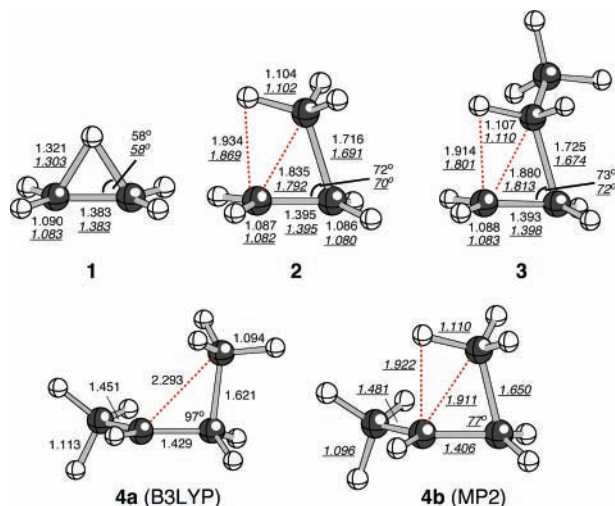


**Figure 2.** Optimized geometries of  $C_2H_5^+$  (**1**),  $C_3H_7^+$  (**2**), and  $C_4H_9^+$  (**3–4**) cations. Selected distances are shown in Å [B3LYP/6-31+G(d,p) in normal text; MP2/6-31+G(d,p) in underlined italics].

As expected, optimizations on  $C_2H_5^+$  led to the bridged structure **1**.<sup>28,29</sup> For both the primary  $C_3H_7^+$  and  $C_4H_9^+$  cations, analogous bridged minima, **2** and **3**, were located. Structures **2** and **3** are extremely similar to each other; the addition of the extra methyl group in **3** has only a small effect.

While B3LYP and MP2 gave similar results for structures **1–3**, they led to somewhat different structures for the secondary  $C_4H_9^+$  cation. At the B3LYP/6-31+G(d,p) level, optimizations on various rotamers (involving different orientations of the potentially bridging methyl group) consistently led to structure **4a**. Although benefiting from significant hyperconjugation (note the  $> 1.6$  Å C–C bond length and the  $97^\circ$  C–C–C angle), this cation does not bridge significantly. Optimizations with MP2/

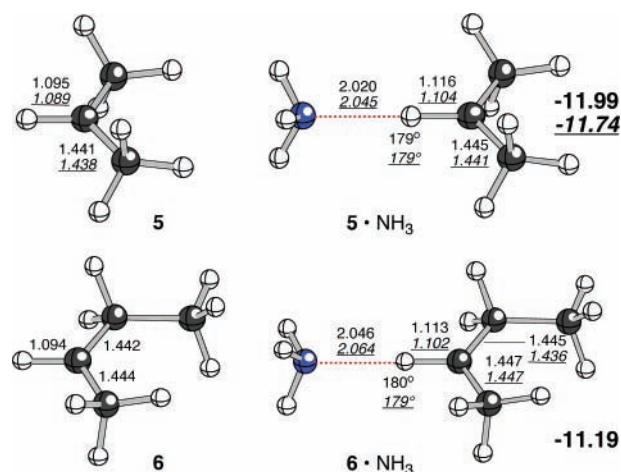


**Figure 3.** Optimized geometries of representative classical cations and their complexes with ammonia. Selected distances are shown in Å, and computed interaction energies are shown to the right of each complex in kcal/mol [B3LYP/6-31+G(d,p) in normal text, MP2/6-31+G(d) in underlined italics].<sup>32</sup>

6-31+G(d,p), however, did lead to a methyl-bridged structure, **4b**, in which the methyl group is rotated with respect to that in **4a** so that one C–H bond can interact weakly with the secondary cation site. Reoptimizing **4b** with B3LYP/6-31+G(d,p) led back to **4a** and reoptimizing **4a** with MP2/6-31+G(d,p) led back to **4b**. Apparently, the two methods differ slightly in their assessment of the abilities of methyl groups to stabilize cationic centers through hyperconjugation and bridging.<sup>30</sup> It is worth noting, however, that hyperconjugation and bridging are not entirely different but can be viewed as different points along a continuum describing the interaction of a carbocationic center with a neighboring C–C bond.<sup>31</sup>

**Complexes with Ammonia.** Next, we examined complexes of these carbocations with  $NH_3$ . First, for comparison, consider the complexes of  $NH_3$  with the classical secondary propyl (**5**) and butyl (**6**) cations shown in Figure 3. Not surprisingly, C–H bonds on electron deficient carbocationic centers seem to be competent C–H hydrogen bond donors. The structures of the carbocations are only very slightly perturbed upon complexation, and  $N\cdots H-C$  distances in these complexes are fairly short. For comparison, computed  $N\cdots H-C$  distances in  $H_3N\cdots H-C_{alkene}$ ,  $H_3N\cdots H-C_{alkyne}$ ,  $H_3N\cdots H-CN$ ,  $H_3N\cdots H-CF_3$ ,  $H_3N\cdots H-C_{1,2,4,5-tetrafluorobenzene}$ , and  $H_3N\cdots H-C_{pentachlorocyclopropane}$  complexes are reported to be  $\sim 2.5$ – $2.7$ ,<sup>5a,d</sup>  $\sim 2.3$ ,<sup>5a,d</sup>  $\sim 2.1$ ,<sup>5b</sup>  $\sim 2.4$ ,<sup>5c</sup>  $\sim 2.2$ ,<sup>5f</sup> and  $\sim 2.2$  Å,<sup>5g</sup> respectively. Computed interaction energies for the carbocation $\cdot NH_3$  complexes in Figure 3 are  $-11$ – $12$  kcal/mol. These values are larger in magnitude than those computed previously for uncharged  $N\cdots H-C$  interactions, which range from approximately  $-1$  kcal/mol for simple  $H_3N\cdots H-C_{alkene}$  complexes to approximately  $-5$  kcal/mol for  $H_3N\cdots H-CN$ .<sup>5a–g</sup>

Similarly, small geometric perturbations and large interaction energies were observed for complexes of ammonia with nonclassical ions. Structures of complexes with cations **1–4** (Figure 2) are shown in Figures 4–7, along with their computed gas phase interaction energies.

For structure **1**, there are two types of nonequivalent hydrogens: the bridging hydrogen and the other four. Allowing ammonia to interact with the bridging hydrogen, as expected, results in deprotonation. Aligning the ammonia lone pair with the other C–H bonds leads, upon geometry optimization, to the complex shown at the left of Figure 4 in which a significant  $N\cdots H-C$  interaction is again observed. Although the symmetry

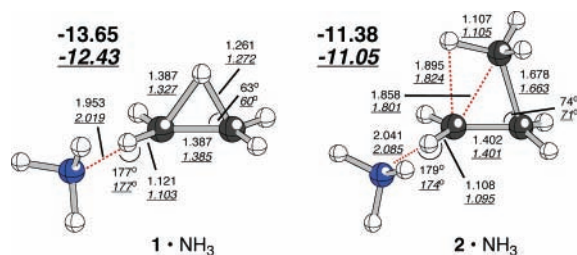
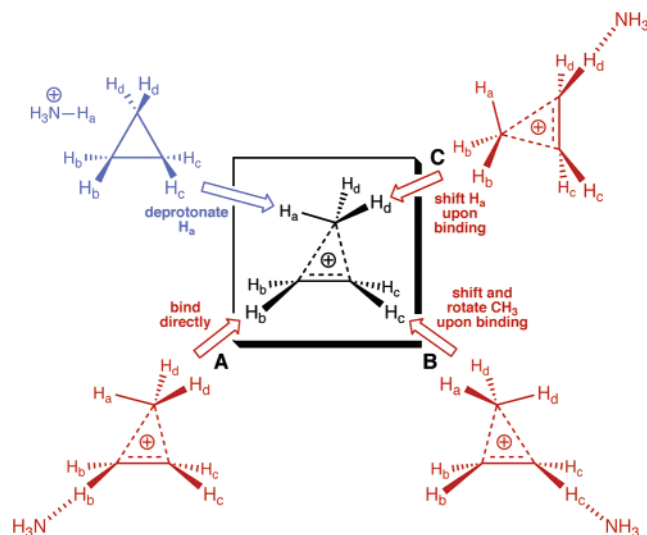


**Figure 4.** Optimized geometries of complexes of cations **1** and **2** with ammonia. Selected distances are shown in Å, and computed interaction energies are shown to the left of each complex in kcal/mol [B3LYP/6-31+G(d,p)].

### SCHEME 1



of the bridging interaction is lost—the distortion reflects the donation of electron density by ammonia to one side of the cation, thus slightly reducing the “electron demand”<sup>33</sup> of that site—bridging still persists.

A similar complex is observed for cation **2** (Figure 4, right). Despite the presence of four types of nonequivalent hydrogens in **2**, only this complex is observed. Interaction of ammonia with  $H_a$  (Scheme 1, blue) leads to deprotonation and cyclopropane formation. Interaction of ammonia with any of the other hydrogens in **2**, however, leads to the complex shown in Figure 4 (Scheme 1, red). Binding of ammonia to either of protons  $H_b$  (interaction **A**) leads directly to the complex shown (or its enantiomer). Binding to protons  $H_c$  (interaction **B**) leads to an equivalent complex by slightly shifting and rotating the bridging methyl group. Binding to protons  $H_d$  again leads to an equivalent complex, in this case via shifting of  $H_a$ . These geometric changes allow the ammonia lone pair to interact with the group that is least involved in bridging. In other words, the donation of electron density from the ammonia helps to stabilize one corner of the protonated cyclopropane unit, allowing the rest of the structure to redistribute its electron density and charge in the most favorable way.

The nature of the binding for the  $2 \cdot \text{NH}_3$  complex, as a representative example, was examined in more detail. First, the interaction energy for the  $2 \cdot \text{NH}_3$  complex was analyzed using the Morokuma–Ziegler decomposition scheme.<sup>34</sup> This analysis indicates that electrostatic interactions contribute approximately twice as much as do orbital interactions to the binding energy for  $2 \cdot \text{NH}_3$ . In addition, the distance and angular dependence of the  $2 \cdot \text{NH}_3$  interaction were probed through two relaxed potential energy scans [using B3LYP/6-31+G(d,p)]. In the first, the

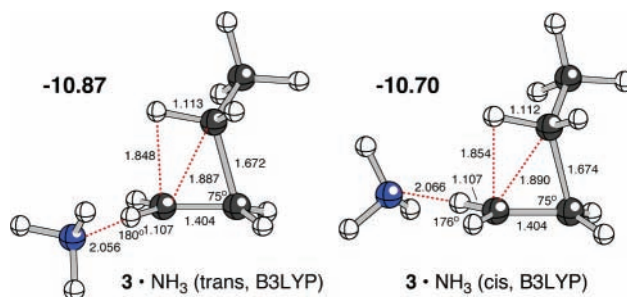


**Figure 5.** Optimized geometries of complexes of cation **3** with ammonia. Selected distances are shown in Å, and computed interaction energies are shown to the left of each complex in kcal/mol [B3LYP/6-31+G(d,p)].

$\text{N} \cdots \text{H}-\text{C}$  angle was held constant at  $179^\circ$  (its value in the fully optimized  $2 \cdot \text{NH}_3$  complex) and the  $\text{N} \cdots \text{H}$  distance was varied from 1.75 to 3.00 Å in 0.25 Å increments while the remainder of the complex was allowed to relax. The  $2 \cdot \text{NH}_3$  binding energy was most favorable at 2.00 Å (note that the optimized  $\text{N} \cdots \text{H}$  distance for this complex is 2.04 Å, as shown in Figure 4) and decreased steadily as the distance was increased from this value (at 3.00 Å, the binding energy was 4.6 kcal/mol less favorable than at 2.00 Å). As the  $\text{N} \cdots \text{H}$  distance was increased, the  $\text{H}-\text{C}$  distance decreased slightly (to 1.088 Å at a  $\text{N} \cdots \text{H}$  distance of 3.00 Å) and the bridging  $\text{CH}_3$  group moved slightly closer to the carbon involved in the  $\text{N} \cdots \text{H}-\text{C}$  interaction (the  $\text{C} \cdots \text{C}$  distance decreased by a maximum of  $\sim 0.03$  Å). In the second scan, the  $\text{N} \cdots \text{H}$  distance was held constant at 2.04 Å (its value in the fully optimized  $2 \cdot \text{NH}_3$  complex) and the  $\text{N} \cdots \text{H} \cdots \text{C}$  (of the  $\text{CH}_2$  group not directly involved in the  $\text{N} \cdots \text{H}-\text{C}$  interaction) angle was varied from 115 to  $175^\circ$  while the remainder of the complex was allowed to relax; this allowed the  $\text{NH}_3$  group to sample different positions around the  $\text{H}-\text{C}$  group while not deviating significantly from the approximate plane in which the  $\text{N} \cdots \text{CH}_2-\text{CH}_2$  substructure resides. Over the range of angles explored, the maximum change in the binding energy was only 1.0 kcal/mol and no significant changes to bond distances were observed.

Interaction of ammonia with cation **3** (Figure 2) is similar to that for **2**. In cation **3**, all nine protons are nonequivalent. Interaction of ammonia with either of the protons of the methylene group in the bridging ethyl unit leads to deprotonation and methylcyclopropane formation. Interaction with the protons on the terminal methylene leads to the complexes shown in Figure 5, which differ in the relative positions of the ammonia and methyl groups (cis or trans). Binding to the protons of the internal (nonbridging) methylene group leads to the same complexes via slight shifting and rotation of the ethyl group as described above for the methyl group of cation **2**. The interaction energies for the two complexes in Figure 5 are of a slightly smaller magnitude than that for the  $2 \cdot \text{NH}_3$  complex, probably as a result of the inherent stabilization of the cation (through hyperconjugation and/or polarization) provided by the appended methyl group in **3**. MP2/6-31+G(d,p) calculations on these  $3 \cdot \text{NH}_3$  complexes lead, via movement of the bridging hydrogen, to the **4b** complexes discussed below.

Binding to cations **4a** and **4b** is more complicated. Optimized structures for  $4a \cdot \text{NH}_3$  and  $4b \cdot \text{NH}_3$  complexes are shown in Figures 6 and 7, respectively. It is perhaps easiest to make sense of these complexes by considering the various complexation sites in **4b** (drawn below). Let's first consider the B3LYP/6-31+G(d,p) results. Interaction of  $\text{NH}_3$  with  $H_a$  leads to the  $4a \cdot \text{NH}_3$  (methine) complex shown in Figure 6; no analogous complex of **4b** (i.e., with the bridging methyl rotated) could be

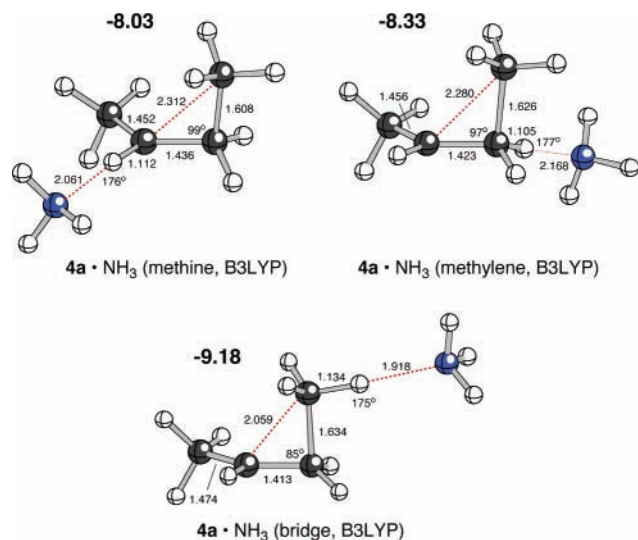


**Figure 6.** Optimized geometries of complexes of cation **4a** with ammonia. Selected distances are shown in Å, and computed interaction energies are shown to the left of each complex in kcal/mol [B3LYP/6-31+G(d,p)].

found at the B3LYP/6-31+G(d,p) level. Interaction of  $\text{NH}_3$  with  $\text{H}_b$  leads to the **4b**· $\text{NH}_3$  (methylene) complex shown in Figure 7; in this case, no analogous complex of **4a** could be found. Interaction of  $\text{NH}_3$  with  $\text{H}_c$  leads to the **4a**· $\text{NH}_3$  (methylene) complex shown in Figure 6 and interaction of  $\text{NH}_3$  with either  $\text{H}_d$  or  $\text{H}_e$  leads to the **4a**· $\text{NH}_3$  (bridge) complex shown in Figure 6. In short, small changes to the conformation of the bridging methyl group occur readily, allowing complexes of types **4a** and **4b** to both form. Remarkably, interaction of  $\text{NH}_3$  with  $\text{H}_f$  does not lead to deprotonation, instead leading to the **4b**· $\text{NH}_3$  (bridge-in) complex shown in Figure 7. When these various structures were sought at the MP2/6-31+G(d,p) level, only **4b**· $\text{NH}_3$  (methine) and **4b**· $\text{NH}_3$  (bridge-out) structures (Figure 7) or methylcyclopropane· $\text{NH}_4^+$  complexes could be found.

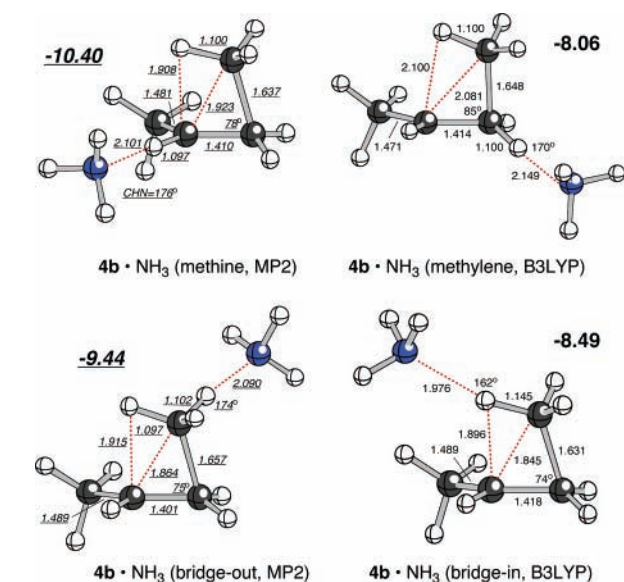
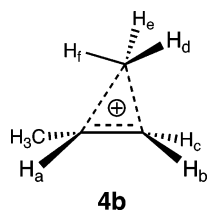


**Figure 7.** Optimized geometries of complexes of cation **4b** with ammonia. Selected distances are shown in Å, and computed interaction energies are shown next to each complex [B3LYP/6-31+G(d,p) in bold; MP2/6-31+G(d,p) in bold underlined italics]. MP2 interaction energies are relative to free **4b** and ammonia while B3LYP interaction energies are relative to free **4a** and ammonia.

**TABLE 1: Computed Interaction Energies [B3LYP/6-31+G(d,p)] for Complexes in Figures 3–7 (the CPCM Method with UAKS Radii Was Used for Solvation Calculations with Dielectric Constants of 2.247, 38.2, and 78.39 for Benzene, Nitromethane, and Water, Respectively)**

complex	interaction energy (kcal/mol)			
	gas phase	benzene	nitromethane	water
<b>1</b> · $\text{NH}_3$	-13.65	-5.67	-0.49	+6.73
<b>2</b> · $\text{NH}_3$	-11.38	-6.69	-3.12	+0.12
<b>3</b> · $\text{NH}_3$ (trans)	-10.87	-6.36	-2.72	+0.50
<b>3</b> · $\text{NH}_3$ (cis)	-10.70	-6.30	-3.00	+0.32
<b>4a</b> · $\text{NH}_3$ (methine)	-8.03	-6.47	-2.76	+1.28
<b>4a</b> · $\text{NH}_3$ (methylene)	-8.33	-4.57	-1.73	+0.84
<b>4a</b> · $\text{NH}_3$ (bridge)	-9.18	-5.16	-1.93	+0.62 <sup>a</sup>
<b>4b</b> · $\text{NH}_3$ (methylene)	-8.06 <sup>b</sup>	<i>c</i>	<i>c</i>	<i>c</i>
<b>4b</b> · $\text{NH}_3$ (bridge-in)	-8.49 <sup>b</sup>	-3.83 <sup>b</sup>	<i>d</i>	+0.90 <sup>b</sup>
<b>5</b> · $\text{NH}_3$	-11.99	-6.94	-3.01	+1.17
<b>6</b> · $\text{NH}_3$	-11.19	-6.40	-3.68	+1.24

<sup>a</sup> This structure has a small imaginary frequency ( $-22\text{ cm}^{-1}$ ) corresponding to rotation of the  $\text{CH}_3\cdots\text{NH}_3$  substructure. Because of the flatness of the energy surface near this structure, we were unable to locate a discrete minimum. <sup>b</sup> Binding energies vs free **4a**. <sup>c</sup> See ref 35. <sup>d</sup> Went to  $\text{NH}_4^+$ ·methylcyclopropane complex.

Overall, while various C–H and C–C bond lengths in carbocations **1–4** change slightly upon complexation, intact nonclassical species do indeed persist in many cases. The  $\text{N}\cdots\text{H}-\text{C}$  interaction energies for these complexes are considerable, comparable to those for  $\text{NH}_3$ ·classical cation complexes and generally at least double in magnitude those computed for overall neutral  $\text{N}\cdots\text{H}-\text{C}$  interactions.<sup>5a–g</sup> The portions of the potential energy surfaces near these minima are extremely flat, however, and estimated barriers for addition of  $\text{NH}_3$  or deprotonation are generally quite small ( $\leq 1$  kcal/mol), but a similar situation also exists for classical cations.

**Solvent Effects.** The structures shown in Figures 2–7 were also examined using continuum solvation calculations [CPCM-(UAKS)-B3LYP/6-31+G(d,p)].<sup>16,17</sup> Dielectric constants corresponding to benzene, nitromethane, and water were used to survey a wide range of solvent polarity. In general, only very small structural changes were observed when the gas phase structures were reoptimized in solvent. Except for the few cases in which deprotonation occurred, changes to the C–C and C–H

distances were all less than  $0.06\text{ \AA}$  and changes to  $\text{N}\cdots\text{H}-\text{C}$  distances were all less than  $0.09\text{ \AA}$ ; most changes were considerably smaller than these maximum values (see Supporting Information for geometries).<sup>35</sup> Interaction energies for these complexes (Table 1) were reduced in magnitude as the polarity of the surrounding environment increased, as expected given that the  $\text{N}\cdots\text{H}-\text{C}$  interactions in question are primarily electrostatic in nature.<sup>3,4a</sup>

**Potential Biological Implications.** Terpenoid synthases produce a plethora of polycyclic natural products from only a few acyclic precursors.<sup>2</sup> In doing so, they control both the regio- and stereoselectivity of various carbon–carbon bond forming and rearrangement reactions with apparent ease, often solving several regio- and stereochemical problems in a single enzyme-catalyzed transformation. The mechanisms of these impressive enzyme-catalyzed polycyclization reactions have been discussed for decades, and many mechanistic proposals have led to elegant

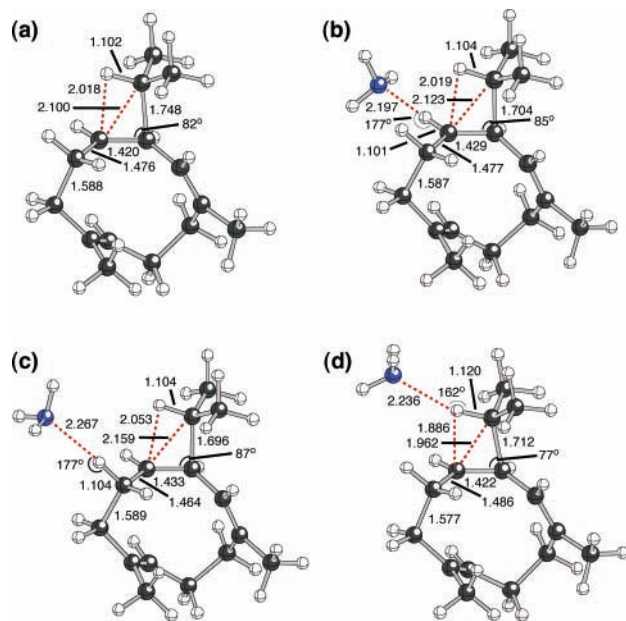


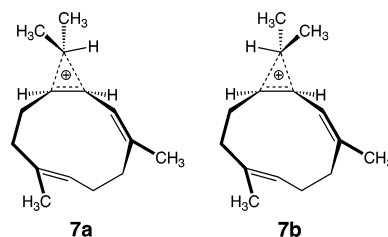
**Figure 8.** Compound **7b** (a) and its  $\text{NH}_3$  complexes (b–d). Selected distances are shown in Å, and computed interaction energies for (b–d) are  $-8.98$ ,  $-8.26$ , and  $-6.96$  kcal/mol, respectively [B3LYP/6-31+G(d,p)], in the gas phase.<sup>39</sup>

biomimetic syntheses of terpenoids and related polycycles.<sup>2,36</sup> Most proposed mechanisms involve the attack of  $\pi$ -bonds onto carbocations and the interconversion of carbocations via [1,2]-sigmatropic shifts and transannular shifts of hydrogen.

An unanswered question in this field is when and where nonclassical carbocations<sup>1</sup> are involved in terpenoid synthase mechanisms. Although the intermediacy of nonclassical species has been suggested by various investigators,<sup>37–39</sup> many mechanistic proposals still focus on the interconversion of classical carbocations. Many studies on simple analogues of biologically relevant carbocations have been reported,<sup>26,37c,f</sup> but the effects of surrounding enzyme active sites on cation structures and rearrangement barriers have not been systematically explored.<sup>26a,c,d,g,i</sup> Nonclassical carbocations are common in nonpolar environments such as the gas phase and have even been shown to exist in aqueous solution.<sup>1,22a</sup> It is reasonable, therefore, to think that they may also exist in enzyme active sites, especially in the relatively nonpolar active sites of terpenoid synthases, which are typically lined with aromatic and other hydrophobic residues.<sup>18</sup> Some terpenoid synthase active sites also contain residues that have hydrogen bond donor and acceptor groups such as histidine, tyrosine, tryptophan, and asparagine,<sup>18</sup> so various types of enzyme–nonclassical cation interactions are possible (Figure 1).

The calculations described above indicate that nonclassical cations can exist in the presence of basic groups and that  $\text{N}\cdots\text{H}-\text{C}$  interactions are associated with significant binding energies. Enzyme active sites, even when lined with hydrophobic and aromatic residues, are not homogeneous. Even so, the continuum solvation calculations described above using benzene as the solvent provide a reasonable model of a nonpolar environment, and the strengths of  $\text{N}\cdots\text{H}-\text{C}$  interactions in this environment typically range from  $-5$  to  $-7$  kcal/mol (Table 1). Although the potential energy surfaces around the nonclassical cation $\cdots$ ammonia complexes are relatively flat, enzymes are skilled at preorganization and could possibly protect nonclassical structures from addition or deprotonation by limiting the movements of potential nucleophiles and bases. This issue will require further study, however.

Recently, He and Cane discussed the possibility that nonclassical cations such as **7a** are involved in germacadienol/germacrene D synthase mechanisms.<sup>37e</sup> To test whether nonclassical species are also viable for large and somewhat conformationally constrained species such as these, we examined structures related to **7a** and their complexes with  $\text{NH}_3$ . B3LYP/6-31+G(d,p) calculations indicate that **7a** is not a minimum in the gas phase (attempted optimization led to species with allylic cation substructures), but the closely related **7b** is (Figure 8a). Several complexes between **7b** and  $\text{NH}_3$  were located, each involving slight changes to the carbocation geometry but maintaining its nonclassical structure overall, even when the  $\text{NH}_3$  interacts directly with hydrogens whose removal (deprotonation) would lead to cyclopropanes or alkenes; representative structures are shown in Figure 8b–d.<sup>40</sup> Much additional work will be required to arrive at a complete picture of this mechanism, but our calculations suggest that if such carbocations are indeed formed in the active site of the enzyme, they may participate in favorable noncovalent interactions with active site residues.



## Conclusions

Overall, our calculations indicate that interactions between nonclassical cations and amines are energetically favorable and their interaction energies are in the range of those for more traditional hydrogen bonds. In addition, structural perturbations to nonclassical structures upon interaction are often minimal. In short, carbocations (both carbonium and carbenium ions) appear to be competent hydrogen bond donors. Further studies on other carbocations and other model enzyme residues are in progress.

**Acknowledgment.** We gratefully acknowledge the University of California, Davis, the donors of the American Chemical Society Petroleum Research Fund, the National Science Foundation CAREER program, and the National Science Foundation's Partnership for Advanced Computational Infrastructure (Pittsburgh Supercomputer Center) for support.

**Supporting Information Available:** Coordinates and energies for all structures and details on the energy decomposition analysis for the  $\mathbf{2}\cdot\text{NH}_3$  complex. This material is available free of charge via the Internet at <http://pubs.acs.org>.

## References and Notes

- (1) For leading references, see (a) Issue 12 of *Acc. Chem. Res.* **1983**, *16*. (b) Brown, H. C. (with comments by Schleyer, P. v. R.) *The Nonclassical Ion Problem*; Plenum: New York, 1977. (c) Olah, G. A.; Laali, K. K.; Wang Q.; Prakash, S. G. K. *Onium Ions*; Wiley-Interscience: New York, 1998.
- (2) For leading references, see (a) Cane, D. E. *Chem. Rev.* **1990**, *90*, 1089–1103. (b) Wendt, K. U.; Schulz, G. E.; Corey, E. J.; Liu, D. R. *Angew. Chem., Int. Ed.* **2000**, *39*, 2812–2833. (c) Abe, I.; Rohmer, M.; Prestwich, G. D. *Chem. Rev.* **1993**, *93*, 2189–2206.
- (3) (a) For a recent example and leading references on  $\text{C}-\text{H}\cdots\text{X}$  ( $\text{X} = \text{N}, \text{O}$ ) interactions in biological systems, see Pierce, A. C.; ter Haar, E.; Binch, H. M.; Kay, D. P.; Patel, S. R.; Li, P. *J. Med. Chem.* **2005**, *48*, 1278–1281. (b) Calhorda, M. J. *Chem. Commun.* **2000**, 801–809.

(4) Recent computations and leading references on C–H···O interactions include (a) Raymo, F. M.; Bartberger, M. D.; Houk, K. N.; Stoddart, J. F. *J. Am. Chem. Soc.* **2001**, *123*, 9264–9267 (this paper discusses C–H···O interactions where the C–H units are part of pyridinium cations). (b) Munshi, P.; Guru Row, T. N. *J. Phys. Chem. A* **2005**, *109*, 659–672. (c) Castellano, R. K. *Curr. Org. Chem.* **2004**, *8*, 845–865. (d) For a proposal on referring to C–H···O interactions as “hydrogen bridges”, see Desiraju, G. R. *Chem. Commun.* **2005**, 2995–3001.

(5) Recent computations on C–H···N interactions: (a) Wetmore, S. D.; Schofield, R.; Smith, D. M.; Radom, L. *J. Phys. Chem. A* **2001**, *105*, 8718–8726 and references therein. (b) Moore Plummer, P. L. *J. Phys. Chem. B* **2004**, *108*, 19582–19588. (c) Herrebout, W. A.; Melikova, S. M.; Delanoye, S. N.; Rutkowski, K. S.; Shchepkin, D. N.; van der Veken, J. *J. Phys. Chem. A* **2005**, *109*, 3038–3044. (d) Domagala, M.; Grabowski, S. J. *J. Phys. Chem. A* **2005**, *109*, 5683–5688. (e) Millar, L. J.; Ford, T. A. *J. Mol. Struct.* **2005**, *744–747*, 195–205. (f) Venkatesan, V.; Fujii, A.; Mikami, N. *Chem. Phys. Lett.* **2005**, *409*, 57–62. (g) Baker, A. B.; Samet, C.; Lyon, J. T.; Andrews, L. *J. Phys. Chem. A* **2005**, *109*, 8280–8289. X-ray structures of complexes with short C–H···N contacts (<2.5 Å) are described in (h) Mascall, M. *Chem. Commun.* **1998**, 303–304. (i) Cotton, F. A.; Daniels, L. M.; Jordan, G. T., IV; Murillo, C. A. *Chem. Commun.* **1997**, 1673–1674.

(6) Frisch, M. J.; Trucks, G. W.; Schlegel, H. B.; Scuseria, G. E.; Robb, M. A.; Cheeseman, J. R.; Montgomery, J. A., Jr.; Vreven, T.; Kudin, K. N.; Burant, J. C.; Millam, J. M.; Iyengar, S. S.; Tomasi, J.; Barone, V.; Mennucci, B.; Cossi, M.; Scalmani, G.; Rega, N.; Petersson, G. A.; Nakatsuji, H.; Hada, M.; Ehara, M.; Toyota, K.; Fukuda, R.; Hasegawa, J.; Ishida, M.; Nakajima, T.; Honda, Y.; Kitao, O.; Nakai, H.; Klene, M.; Li, X.; Knox, J. E.; Hratchian, H. P.; Cross, J. B.; Bakken, V.; Adamo, C.; Jaramillo, J.; Gomperts, R.; Stratmann, R. E.; Yazyev, O.; Austin, A. J.; Cammi, R.; Pomelli, C.; Ochterski, J. W.; Ayala, P. Y.; Morokuma, K.; Voth, G. A.; Salvador, P.; Dannenberg, J. J.; Zakrzewski, V. G.; Dapprich, S.; Daniels, A. D.; Strain, M. C.; Farkas, O.; Malick, D. K.; Rabuck, A. D.; Raghavachari, K.; Foresman, J. B.; Ortiz, J. V.; Cui, Q.; Baboul, A. G.; Clifford, S.; Cioslowski, J.; Stefanov, B. B.; Liu, G.; Liashenko, A.; Piskorz, P.; Komaromi, I.; Martin, R. L.; Fox, D. J.; Keith, T.; Al-Laham, M. A.; Peng, C. Y.; Nanayakkara, A.; Challacombe, M.; Gill, P. M. W.; Johnson, B.; Chen, W.; Wong, M. W.; Gonzalez, C.; Pople, J. A. *Gaussian 03*, revision C.02; Gaussian, Inc.: Wallingford, CT, 2004.

(7) (a) Becke, A. D. *J. Chem. Phys.* **1993**, *98*, 5648–5652. (b) Becke, A. D. *J. Chem. Phys.* **1993**, *98*, 1372–1377. (c) Lee, C.; Yang, W.; Parr, R. G. *Phys. Rev. B* **1988**, *37*, 785–789. (d) Stephens, P. J.; Devlin, F. J.; Chabalowski, C. F.; Frisch, M. J. *J. Phys. Chem.* **1994**, *98*, 11623–11627. (8) Möller, C.; Plesset, M. S. *Phys. Rev.* **1934**, *46*, 618–622.

(9) (a) Vrcek, I. V.; Vrcek, V.; Siehl, H.-U. *J. Phys. Chem. A* **2002**, *106*, 1604–1611. (b) Farcasiu, D.; Lukinskas, P.; Pamidighantam, S. V. *J. Phys. Chem. A* **2002**, *106*, 11672–11675. (c) Gutta, P.; Tantillo, D. J. *Angew. Chem., Int. Ed.* **2005**, *44*, 2719–2723. (d) Siebert, M. R.; Tantillo, D. J. *J. Org. Chem.* **2006**, *71*, 645–654.

(10) See, for example, (a) Ireta, J.; Neugebauer, J.; Scheffler, M. *J. Phys. Chem. A* **2004**, *108*, 5692–5698. (b) Zhou, Z.; Shi, Y.; Zhou, X. *J. Phys. Chem. A* **2004**, *108*, 813–822.

(11) Chalasinski, G.; Szczesniak, M. M. *Chem. Rev.* **2000**, *100*, 4227–4252.

(12) Lynch, B. J.; Zhao, Y.; Truhlar, D. G. *J. Phys. Chem. A* **2003**, *107*, 1384–1388.

(13) (a) Peng, C.; Schlegel, H. B. *Isr. J. Chem.* **1993**, *33*, 449–454. (b) Peng, C.; Ayala, P. Y.; Schlegel, H. B.; Frisch, M. J. *J. Comput. Chem.* **1996**, *14*, 49–56.

(14) (a) Gonzalez, C.; Schlegel, H. B. *J. Phys. Chem.* **1990**, *94*, 5523–5527. (b) Fukui, K. *Acc. Chem. Res.* **1981**, *14*, 363–368.

(15) Boys, S. F.; Bernardi, F. *Mol. Phys.* **1970**, *19*, 553–566.

(16) (a) Barone, V.; Cossi, M. *J. Phys. Chem. A* **1998**, *102*, 1995–2001. (b) Cossi, M.; Rega, N.; Scalmani, G.; Barone, V. *J. Comput. Chem.* **2003**, *24*, 669–681.

(17) Takano, Y.; Houk, K. N. *J. Chem. Theor. Comput.* **2005**, *1*, 70–77.

(18) (a) Greenhagen, B.; Chappell, J. *Proc. Natl. Acad. Sci. U.S.A.* **2001**, *98*, 13479–13481. (b) Starks, C. M.; Back, K.; Chappell, J.; Noel, J. P. *Science* **1997**, *277*, 1815–1820. (c) Lesburg, C. A.; Zhai, G.; Cane, D. E.; Christianson, D. W. *Science* **1997**, *277*, 1820–1824. (d) Caruthers, J. M.; Kang, I.; Rynkiewicz, M. J.; Cane, D. E.; Christianson, D. W. *J. Mol. Biol.* **2000**, *275*, 25533–25539. (e) Rynkiewicz, M. J.; Cane, D. E.; Christianson, D. W. *Proc. Natl. Acad. Sci. U.S.A.* **2001**, *98*, 13543–13548. (f) Rynkiewicz, M. J.; Cane, D. E.; Christianson, D. W. *Biochemistry* **2002**, *41*, 1732–1741. (g) Whittington, D. A.; Wise, M. L.; Urbansky, M.; Coates, R. M.; Croteau, R. B.; Christianson, D. W. *Proc. Natl. Acad. Sci. U.S.A.* **2002**, *99*, 15375–15380. (h) Lesburg, C. A.; Caruthers, J. M.; Paschall, C. M.; Christianson, D. W. *Curr. Opin. Struct. Biol.* **1998**, *8*, 695–703.

(19) Müller, N.; Falk, A. *Ball & Stick V.3.7.6*; molecular graphics application for MacOS computers; Johannes Kepler University: Linz, 2000.

(20) The modeling of enzyme···transition structure interactions using quantum mechanical calculations on small models of residues present in

enzyme active sites has been called the “theozyme” approach. For leading references, see (a) Tantillo, D. J.; Chen, J.; Houk, K. N. *Curr. Opin. Chem. Biol.* **1998**, *2*, 743–750. (b) Tantillo, D. J.; Houk, K. N. Theozymes and catalyst design. In *Stimulating Concepts in Chemistry*; Wiley-VCH: Weinheim, Germany, 2000; pp 79–88. (c) Na, J.; Houk, K. N.; Shevlin, C. G.; Janda, K. D.; Lerner, R. A. *J. Am. Chem. Soc.* **1993**, *115*, 8453–8454. (d) Müller, C.; Wang, L.-H.; Zipse, H. Enzymes, abzymes, chemzymes—Theozymes? In *Transition State Modeling for Catalysis*; Truhlar, D. G., Morokuma, K., Eds.; ACS Symposium Series 721; American Chemical Society: Washington, DC, 1999; pp 61–73.

(21) Breneman, C. M.; Wiberg, K. B. *J. Comput. Chem.* **1990**, *11*, 361–373.

(22) Computations on complexes of nonclassical cations with potential hydrogen bond acceptors have only rarely been described. (a) 2-Norbornyl cation + water: Schreiner, P. R.; Severance, D. L.; Jorgensen, W. L.; Schleyer, P. v. R.; Schaefer, H. F., III. *J. Am. Chem. Soc.* **1995**, *117*, 2663–2664 and references therein. (b) Edge-protonated cubane + dimethyl ether: Fokin, A. A.; Tkachenko, B. A.; Gunchenko, P. A.; Schreiner, P. R. *Angew. Chem., Int. Ed.* **2005**, *44*, 146–149. (c) C<sub>3</sub>H<sub>7</sub><sup>+</sup> + I<sup>−</sup>: Park, S. T.; Kim, S. K.; Kim, M. S. *Nature* **2002**, *415*, 306–308. (d) C<sub>3</sub>H<sub>7</sub><sup>+</sup> + zeolite models (transition states, not minima): Frash, M. V.; Kazansky, V. B.; Rigby, A. M.; van Santen, R. A. *J. Phys. Chem. B* **1997**, *101*, 5346–5351. (e) See also refs 26a,d,g.

(23) Computations on complexes of classical cations with potential hydrogen bond acceptors include the following: (a) Cyclohexadienyl cation + water: Kryachko, E. S.; Nguyen, M. T. *J. Phys. Chem. A* **2001**, *105*, 153–155. (b) Benzyl and other alkyl cations + methanol: Hori, K.; Sonoda, T.; Harada, M.; Yamazaki-Nishida, S. *Tetrahedron* **2000**, *56*, 1429–1436. (c) Substituted cyclohexadienyl cations + zeolite models: Arstad, B.; Kolboe, S.; Swang, O. *J. Phys. Chem. B* **2004**, *108*, 2300–2308. (d) Tertiary carbocation + methanol: Filippi, A. *Chem. Eur. J.* **2003**, *9*, 5396–5403. (e) Benzene radical cation + water(s): Ibrahim, Y. M.; Meot-Ner (Mautner), M.; Alshraeh, E. H.; El-Shall, M. S.; Scheiner, S. *J. Am. Chem. Soc.* **2005**, *127*, 7053–7054. (f) See also ref 26.

(24) Computations on complexes of classical cations with  $\pi$ -systems include (a) Miklis, P. C.; Ditchfield, R.; Spencer, T. A. *J. Am. Chem. Soc.* **1998**, *120*, 10482–10489. (b) Filippi, A.; Roselli, G.; Renzi, G.; Grandinetti, F.; Speranza, M. *Chem. Eur. J.* **2003**, *9*, 2072–2078. (c) Berthomieu, D.; Brenner, V.; Ohanessian, G.; Denbez, J. P.; Millié, P.; Audier, H. E. *J. Phys. Chem.* **1995**, *99*, 712–720. (d) Chalk, A. J.; Radom, L. *Int. J. Mass Spectrom.* **2000**, *199*, 29–40. (e) Heidrich, D. *Angew. Chem., Int. Ed.* **2002**, *41*, 3208–3210. (f) Marcantoni, E.; Roselli, G.; Lucarelli, L.; Renzi, G.; Filippi, A.; Trionfetti, C.; Speranza, M. *J. Org. Chem.* **2005**, *70*, 4133–4141. (g) See also ref 26c.

(25) Interactions of cyclopropyl C–H bonds with potential hydrogen bond acceptors (bromocyclopropane + amines): Bedell, B. L.; Goldfarb, L.; Mysak, E. R.; Samet, C.; Maynard, A. *J. Phys. Chem. A* **1999**, *103*, 4572–4579.

(26) Leading references on calculations on enzyme-catalyzed carbocation rearrangements: (a) Rajamani, R.; Gao, J. *J. Am. Chem. Soc.* **2003**, *125*, 12768–12781. (b) Nishizawa, M.; Yadav, A.; Imagawa, H.; Sugihara, T. *Tetrahedron Lett.* **2003**, *44*, 3867–3870. (c) Jensen, C.; Jorgensen, W. L. *J. Am. Chem. Soc.* **1997**, *119*, 10846–10854. (d) Gao, D.; Pan, Y.-K.; Byun, K.; Gao, J. *J. Am. Chem. Soc.* **1998**, *120*, 4045–4046. (e) Vrcek, V.; Saunders, M.; Kronja, O. *J. Org. Chem.* **2003**, *68*, 1859–1866. (f) Hess, B. A., Jr.; Smentek, L. *Org. Lett.* **2004**, *6*, 1717–1720 and references therein. (g) Lee, J. K.; Houk, K. N. *Angew. Chem., Int. Ed. Engl.* **1997**, *36*, 1003–1005. (h) Schulz-Gasch, T.; Stahl, M. *J. Comput. Chem.* **2003**, *24*, 741–753. (i) Oikawa, H.; Nakamura, K.; Tushima, H.; Toyomasu, T.; Sassa, T. *J. Am. Chem. Soc.* **2002**, *124*, 9145–9153. (j) See also ref 9c. (k) Crystal structures of some nonclassical ions with weakly coordinating counterions have been reported. For leading references, see (l) Laube, T. *Chem. Rev.* **1998**, *98*, 1277–1312. (m) Laube, T. *Acc. Chem. Res.* **1995**, *28*, 399–405. (n) Kato, T.; Reed, C. A. *Angew. Chem., Int. Ed.* **2004**, *43*, 2908–2911.

(27) Previous calculations on the cations shown in Figure 2 can be found in (a) Raghavachari, K.; Whiteside, R. A.; Pople, J. A.; Schleyer, P. v. R. *J. Am. Chem. Soc.* **1981**, *103*, 5649–5651. (b) Chiavarino, B.; Crestoni, M. E.; Fokin, A. A.; Fonarini, S. *Chem. Eur. J.* **2001**, *7*, 2916–2921. (c) Koch, W.; Liu, B. P.; Schleyer, P. v. R. *J. Am. Chem. Soc.* **1989**, *111*, 3479–3480. (d) Rio, E. d.; Lopez, R.; Sordo, T. L. *J. Phys. Chem. A* **1998**, *102*, 6831–6834. (e) For slightly larger systems, see Vrcek, V.; Saunders, M.; Kronja, O. *J. Am. Chem. Soc.* **2004**, *126*, 13701–13707.

(28) Bridged C<sub>2</sub>H<sub>5</sub><sup>+</sup> **1** is an isolobal (Hoffmann, R. *Angew. Chem., Int. Ed. Engl.* **1982**, *21*, 711–724) analogue of the organometallic complexes [M(C<sub>2</sub>H<sub>4</sub>)]<sup>+</sup>. See, for example, (a) Stringer, K. L.; Citir, M.; Metz, R. B. *J. Phys. Chem. A* **2004**, *108*, 6996–7002. (b) Dewar, M. J. S.; Ford, G. P. *J. Am. Chem. Soc.* **1979**, *101*, 783–791. (c) Ziegler, T. Rauk, A. *Inorg. Chem.* **1979**, *18*, 1558–1565. (d) Hertwig, R. H.; Koch, W.; Schroeder, D.; Schwarz, H.; Hrusak, J.; Schwerdtfeger, P. *J. Phys. Chem.* **1996**, *100*, 12253–12260.

(29) By constraining one H–C–C angle to 113° to prevent bridging and the H–C–C–H dihedral angles for the other two H's of the methyl

group (fixed to +123 and -123°) and then allowing all of the other degrees of freedom of **1** to relax, we arrived at a structure resembling a classical (nonbridging) ethyl cation; this constrained structure was ~4 kcal/mol higher in energy than **1**.

(30) MP2, as compared to B3LYP, has shown a tendency to more strongly favor delocalized cation structures in other systems as well. See, for example, ref 9.

(31) (a) Olah, G. A. *J. Org. Chem.* **2005**, *70*, 2413–2429. (b) Olah, G. A. *J. Org. Chem.* **2001**, *66*, 5943–5957.

(32) MP2/6-31+G(d,p) data is not shown for **6**, since at this level no uncomplexed classical 2-butyl cation could be located; instead, a *C<sub>s</sub>* symmetric hydrogen-bridged structure was located instead. At the B3LYP/6-31+G(d,p) level, the analogous hydrogen-bridged structure is a transition structure for the degenerate [1,2]-hydrogen shift of **6**; the barrier for this shift at the B3LYP/6-31+G(d,p) level is 1.5 kcal/mol. This is consistent with the tendency for MP2 to have a slightly greater preference for highly delocalized carbocation structures as compared to B3LYP.<sup>9</sup>

(33) Olah, G. A.; Berrier, A. L.; Arvanaghi, M.; Prakash, G. K. S. *J. Am. Chem. Soc.* **1981**, *103*, 1122–1128 and references therein.

(34) The analysis for 2·NH<sub>3</sub> was performed using the B3LYP functional as implemented in ADF2005 and the TZ2P basis set. See Bickelhaupt, F. M.; Baerends, E. J. *Rev. Comput. Chem.* **2000**, *15*, 1–86 for a general description of the use of such methods in ADF (ADF2005; SCM, Theoretical Chemistry, Vrije Universiteit: Amsterdam, The Netherlands, <http://www.scm.com>; te Velde, G.; Bickelhaupt, F. M.; Baerends, E. J.; Fonseca Guerra, C.; van Gisbergen, S. J. A.; Snijders, J. G.; Ziegler, T. *J. Comput. Chem.* **2001**, *22*, 931–967; Fonseca Guerra, C.; Snijders, J. G.; te Velde, G. Baerends, E. J. *Theor. Chem. Acc.* **1998**, *99*, 391–403).

(35) Unlike the other complexes, and in contrast to its gas phase behavior, the 4b·NH<sub>3</sub> (methylene) complex led, upon optimization, to 2-butene·NH<sub>4</sub><sup>+</sup> complexes in all three solvents.

(36) Representative examples include (a) van Tamelen, E. E. *Acc. Chem. Res.* **1975**, *8*, 152–158. (b) Johnson, W. S. *Angew. Chem., Int. Ed. Engl.* **1976**, *15*, 9–17. (c) Zhang, J.; Corey, E. J. *Org. Lett.* **2001**, *3*, 3215–3216 (additional note: *Org. Lett.* **2002**, *4*, 3017).

(37) For leading references on proposed nonclassical intermediates in terpenoid biosynthesis, see (a) Wessjohann, L. A.; Brandt, W. *Chem. Rev.* **2003**, *103*, 1625–1647. (c) Giner, J.-L.; Buzek, P.; Schleyer, P. v. R. *J. Am. Chem. Soc.* **1995**, *117*, 12871–12872. (d) Erickson, H. K.; Poulter, C. D. *J. Am. Chem. Soc.* **2003**, *125*, 6886–6888. (e) He, X.; Cane, D. E. *J. Am. Chem. Soc.* **2004**, *126*, 2678–2679. (f) Dewar, M. J. S.; Ruiz, J. M. *Tetrahedron* **1987**, *43*, 2661–2674. (g) For leading references to older proposals by Djerassi, Arigoni, Ruzicka, Eschenmoser, and others, see Giner, J.-L. *Chem. Res.* **1993**, *93*, 1735–1752.

(38) For a discussion of the possibility of nonclassical ion formation in antibody-catalyzed reactions, see (a) Ma, L.; Sweet, E. H.; Schultz, P. G. *J. Am. Chem. Soc.* **1999**, *121*, 10227–10228 and references therein. (b) Li, T.; Janda, K. D.; Lerner, R. A. *Nature* **1996**, *379*, 326–327. (c) See also ref 26g.

(39) Protonated cyclopropanes have also been proposed as intermediates in the biosynthesis of cyclopropane fatty acids. See, for example, Iwig, D. F.; Grippe, A. T.; McIntyre, T. A.; Booker, S. J. *Biochemistry* **2004**, *43*, 13510–13524.

(40) Computed interaction energies, based on single point calculations in solvent, for (b–d): in benzene, -5.83, -3.96, and -5.87 kcal/mol; in nitromethane, -2.84, -1.26, and -3.68 kcal/mol; and in water, +1.23, +1.64, and -0.66 kcal/mol.